

POTENTIAL OF NON-STANDARD EMITTANCE DAMPING SCHEMES FOR LINEAR COLLIDERS

H.H. Braun, M. Korostelev, F. Zimmermann, CERN, Geneva, Switzerland

Abstract

We estimate the potential of various non-standard schemes for producing low-emittance electron/positron beams in a linear collider and compare their projected performance with that achieved by the present design of the CLIC damping ring. The options considered include the use of rf-wigglers and the integration of radiation damping into the linac.

INTRODUCTION

The 3-dimensional target emittances for the CLIC beam are quite demanding. The present design generates this beam by a conventional damping ring, with a RACETRACK shape. Its circumference is 360 m and the beam energy 2.42 GeV [1]. The ring consists of TME cells in the arcs and 1.634-T wigglers with 20-cm period in the two long straights. The wiggler magnets cover a total length of 167 m. As illustrated in Table 1, for the design bunch population of $N_b=3 \times 10^9$, the present design falls slightly short of the desired 6-dimensional beam density, especially in the vertical plane. Therefore, we here explore two alternative approaches to produce a brilliant low-emittance beam, namely (1) the use of rf wigglers or rf undulators instead of magnetic wigglers in the ring, and (2) the integration of the damping wigglers into the linac. We show that both of these approaches may reach the CLIC target parameters, and that the rf wiggler promises the best performance.

Table 1: Target values and emittances simulated for the present CLIC damping-ring design with quantum excitation, radiation damping, and intrabeam scattering for a bunch population $N_b=3 \times 10^9$.

normalized rms emittance	design goal	achieved with present wiggler-based ring
longitudinal	9.8 mm	8.1 mm
horizontal	450 nm	578 nm
vertical	3 nm	8.1 nm

RF WIGGLER AND RF UNDULATOR

Conventional damping rings operate with wiggler magnets. In this case the quantum excitation scales as the square of the wiggler period. One possibility to reduce the wiggler period is to employ a wiggler based on rf. Depending on the available rf power and breakdown limits, such device may operate as an undulator rather than as a wiggler. The undulator regime is roughly defined by $\lambda_p \hat{B} < 0.01 \text{ T m}$, where \hat{B} denotes the equivalent peak magnetic field. Rf undulators were previously considered by various authors for the purpose of synchrotron-light generation, e.g., in [2,3]. As simple

example, we consider a rectangular waveguide operated in the TE_{10} mode, though more complicated arrangements, such as disk-loaded structures, would provide a better performance. For the TE_{10} waveguide mode the equivalent wiggler period is

$$\lambda_p = \lambda_{rf} / (1 + \sqrt{1 - \omega_c^2 / \omega^2}) \text{ where } \omega_c = \pi c / a. \quad (1)$$

The rf power is tied to the equivalent magnetic field as

$$P_{rf} = \frac{\hat{B}^2 b a \omega k_z}{4(\omega / c + k_z)^2 \mu_0} \text{ with } k_z = \sqrt{(\omega / c)^2 - (\pi / a)^2}. \quad (2)$$

In Fig. 1 the relations (1) and (2) are illustrated as a function of waveguide width a , for an rf power of 200 MW, an rf frequency of 30 GHz, and a fixed waveguide height b . Equivalent fields of about 1 T and wiggler periods of half a centimetre appear feasible.

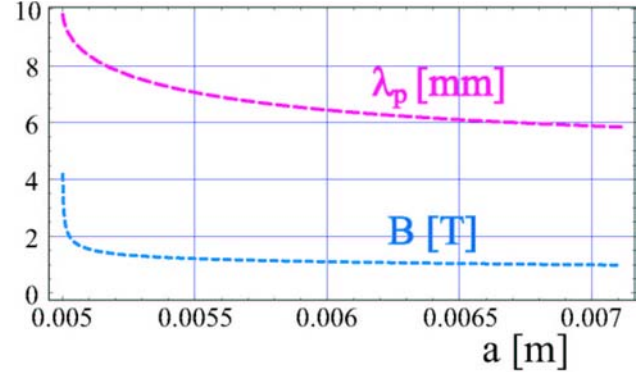


Figure 1: Peak magnetic field (bottom curve) and equivalent wiggler period (top curve) for a TE_{10} mode at 200 MW at 30 GHz, propagating in a waveguide of height $b=2$ mm as a function of the waveguide width a .

For a ring with either wiggler or undulator, the transverse amplitude damping time is $\tau_{x,y} = 4 / (a E \hat{B}_w^2 c)$, where E is the energy in GeV, \hat{B}_w the peak magnetic wiggler field, $a = 2c^2 e^2 r_e (R_w + 2B_d^2 R_d / \hat{B}_w^2) / (3(m_e c^2)^3)$, R_w the wiggler filling factor, B_d the arc dipole field, and R_d the arc dipole filling factor. The equilibrium emittances are determined by the balance of radiation damping, quantum excitation, and intrabeam scattering. The usual quantum excitation and intrabeam scattering in the horizontal plane are proportional to Sand's curly- H function, whose average, for a sinusoidal wiggler field, we approximate as $\langle H \rangle_w \approx \beta \lambda_p^2 (e \hat{B} c)^2 / (8\pi^2 E^2)$, or for a TME arc as $\langle H \rangle_d \approx l_d^3 / \rho_d^2 / (12\sqrt{15}) \epsilon_r$, where l_d and ρ_d are dipole length and bending radius; ϵ_r is the emittance detuning factor. The quantum excitation in the vertical plane, and for an undulator also in the horizontal plane, are

determined by the opening angle effect. For a wiggler, this was computed by Hirata [4] and for an undulator partially by Hofmann [5], and, considering Compton scattering off a laser rather than an rf wave, by Huang and Ruth [6,7]. We approximate the excitation from intrabeam scattering (IBS) by averaging Bane's formula [8], itself a simplification of [9]. Assuming also that $\beta_x \approx \beta_y$ (denoted by β) we can estimate the equilibrium emittances for a damping ring with wiggler as

$$\varepsilon_{N,x} = 2 \frac{b_{1,w}}{a} \left(\beta \lambda_p^2 \hat{B}_w^3 R_w + \frac{\pi^3}{2\sqrt{15}} \varepsilon_r R_d l_d^3 \frac{B_d^3}{B_w^2} \right) + 2 \frac{b_{2,w}}{a} \beta \left(R_w \hat{B}_w + \frac{3\pi}{4} R_d \frac{B_d^3}{B_w^2} \right) + \frac{2h}{aE^{7/2}} \frac{g(\alpha)}{\varepsilon_{N,x}^{3/4} \varepsilon_{N,y}^{3/4} \sigma_s} \left(\lambda_p^2 \beta^{1/2} R_w + (1-R_w) \frac{\varepsilon_r}{\beta^{1/2}} \frac{2\pi^2}{3\sqrt{15}} l_d^2 \frac{B_d^3}{B_w^2} \right)$$

$$\varepsilon_{N,y} = 2 \frac{b_{2,w}}{a} \beta_x \left(R_w \hat{B}_w + \frac{3\pi}{4} R_d \frac{B_d^3}{B_w^2} \right) + \kappa \frac{2h}{aE^{7/2}} \frac{g(\alpha)}{\varepsilon_{N,x}^{3/4} \varepsilon_{N,y}^{3/4} \sigma_s} \left(\lambda_p^2 \beta^{1/2} R_w + (1-R_w) \frac{\varepsilon_r}{\beta^{1/2}} \frac{2\pi^2}{3\sqrt{15}} l_d^2 \frac{B_d^3}{B_w^2} \right)$$

$$\varepsilon_{N,s}^2 = \frac{g_w}{a} E^3 \sigma_s^2 \left(R_w \hat{B}_w + R_d \frac{3\pi}{4} \frac{B_d^3}{B_w^2} \right) + \frac{f}{a} \frac{\sigma_s g(\alpha)}{\beta^{1/2} E^{1/2} \hat{B}^2 \varepsilon_{N,x}^{3/4} \varepsilon_{N,y}^{3/4}}$$

where the coefficients (and functions) are $\kappa \approx 1\%$,

$$b_{1,w} = \frac{55}{288\sqrt{3}\pi^3} \frac{c^6 e^5 r_e \hbar}{(m_e c^2)^7}, \quad b_{2,w} = \frac{13}{36\sqrt{3}\pi} \frac{c^4 e^3 r_e \hbar}{(m_e c^2)^5},$$

$$g_w = \frac{55}{36\sqrt{3}\pi} \frac{c^4 e^3 r_e \hbar}{(m_e c^2)^8}, \quad h = \frac{r_e^2 N_b (\log) e^2 c^2}{64\pi^2} (m_e c^2)^{1/2},$$

$$\alpha = \sqrt{\frac{\beta_x \varepsilon_y}{\beta_y \varepsilon_x}}, \quad g(\alpha) \approx \alpha^{(0.021-0.044 \ln \alpha)}, \quad f = \frac{r_e^2 N_b (\log)}{8(m_e c^2)^{1/2}}.$$

In the undulator regime, the above equations change due to the different photon angular and energy spectrum. Ignoring the arcs and considering an ideal filling factor $R_u \equiv R_w = 1$, the undulator equilibrium emittances are

$$\varepsilon_{N,x} = 2 \frac{b_{1,u}}{a} \beta_x \lambda_p \hat{B}^2 + 2 \frac{b_{2,u}}{a} \beta_x \frac{1}{\lambda_p} + \frac{\lambda_p^2 \beta_x^{3/4}}{\beta_y^{1/4}} \frac{2h}{aE^{9/2}} \frac{g(\alpha)}{\varepsilon_{N,x}^{3/4} \varepsilon_{N,y}^{3/4} \sigma_s}$$

$$\varepsilon_{N,y} = 2 \frac{b_{2,u}}{a} \beta_y \frac{1}{\lambda_p} + \kappa \frac{\lambda_p^2 \beta_x^{3/4}}{\beta_y^{1/4}} \frac{2h}{aE^{9/2}} \frac{g(\alpha)}{\varepsilon_{N,x}^{3/4} \varepsilon_{N,y}^{3/4} \sigma_s}$$

$$\varepsilon_{N,s}^2 = \frac{g_u}{a} \frac{1}{\lambda_p} E^3 \sigma_s^2 + \frac{f}{a} \frac{\sigma_s g(\alpha)}{\beta_x^{1/4} \beta_y^{1/4} E^{1/2} \hat{B}^2 \varepsilon_{N,x}^{3/4} \varepsilon_{N,y}^{3/4}} \text{ where}$$

$$b_{1,u} = \frac{7}{30\pi} \frac{c^4 e^4 r_e}{(m_e c^2)^6} \hbar c, \quad b_{2,u} = \frac{\pi c^2 e^2 r_e}{(m_e c^2)^4} \hbar c, \quad g_u = \frac{7\pi}{15} \hbar c \frac{c^2 e^2 r_e}{(m_e c^2)^7}.$$

Arc contributions would be the same as for the wiggler. Note that the equilibrium-momentum spread without arcs and in the absence of IBS for a pure undulator $\sigma_{\delta,u} = ((7\pi/10)\lambda_e \gamma / \lambda_p)^{1/2}$ differs from that for a pure wiggler $\sigma_{\delta,w} = (55/(24\sqrt{3}\pi)\lambda_e B \gamma / (m_e c))^{1/2}$.

Table 2 lists parameters, damping times, and equilibrium emittances for the present damping ring design, if the magnetic wigglers are replaced either by rf wigglers or by rf undulators at 30 GHz. The numbers include the arc contributions. Figure 2 illustrates the dependence on the effective field of the rf wiggler, computed as in [1].

Table 2: Example parameters for two damping rings, based on either rf wigglers or rf undulators at 30 GHz.

	rf wiggler	rf undulator
rf power	200 MW	50 MW
Waveguide dimensions	2, 5.1 mm	2, 7 mm
Equivalent peak field	1.5 T	0.5 T
Equivalent wave length	8.2 mm	5.9 mm
Parameter $K\lambda$	1.14	0.27
Circumference	357 m	357 m
Total undulator length	160 m	160 m
Beam energy	2.42 GeV	2.42 GeV
Transv. damping time	3.36 ms	11.6 ms
Beta at wiggler/undulator	5 m	5 m
Rms bunch length	2 mm	3 mm
Bunch population	3×10^9	3×10^9
Equilibrium norm. hor. emittance w. (& w/o) IBS	587 nm (73 nm)	924 nm (250 nm)
Equilibrium norm. vertical emittance w. (& w/o) IBS	5.4 nm (0.3 nm)	7.1 nm (0.3 nm)
Equilibrium norm. longit. emittance w. (& w/o) IBS	10.8 mm (7.5 mm)	13.2 mm (9.5 mm)

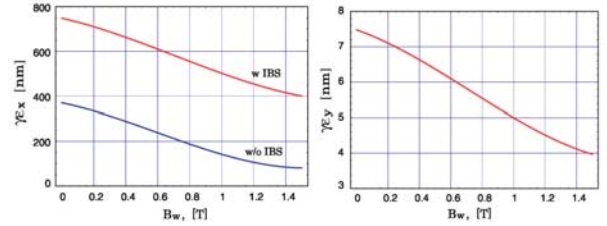


Figure 2: Horizontal and vertical equilibrium emittances (red curves: including IBS) vs. wiggler field for $\lambda_p=8$ mm.

SC WIGGLER IN THE LINAC

A second approach to reach small emittances is to install high-field wigglers along the main linac. Advantages are that there are no arcs contributing to quantum excitation and, at higher energies, intrabeam scattering can be neglected. A disadvantage is the additional linac length and rf power required. Such a scheme was first proposed in [10] for VLEPP, albeit with much larger emittances. For fast damping, superconducting wiggler magnets are needed, whose field we parameterize as

$$B_y = B_0 \cosh\left(\frac{2\pi}{\lambda} y\right) \cos\left(\frac{2\pi}{\lambda} z\right), \quad B_z = B_0 \sinh\left(\frac{2\pi}{\lambda} y\right) \sin\left(\frac{2\pi}{\lambda} z\right)$$

If the field at the gap ($y=g/2, z=0$) shall not exceed a maximum value B_c , the maximum field on axis is

$B_{\max} = \sqrt{2} B_c / \sqrt{1 + \cosh(2\pi g / \lambda)}$. For example, with the full gap $g=3$ mm, and $B_c=10$ T, the maximum field on axis varies with the wiggler period as illustrated in Fig. 3. To operate as an undulator, we would need a small period $\lambda \sim 1$ mm. A field of about 10 T would then imply a full gap of less than 100-200 μm , which is impractical.

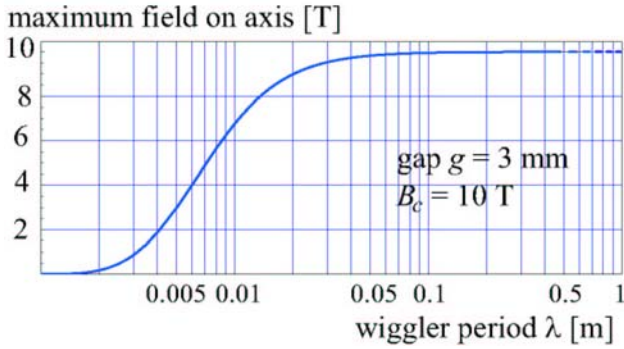


Figure 3: Maximum wiggler field on axis as a function of wiggler period.

The total length of the damping part of the linac is $L_{tot} = 2 \log(\epsilon_{initial} / \epsilon_{final}) [E / G + 1 / (a \hat{B}^2 E)]$ where $\epsilon_{initial}$ and ϵ_{final} denote the initial and final emittances, G the accelerator gradient in units of GeV/m and the factor 2 arises from the difference between longitudinal and transverse damping (for the common partition numbers). Inserting example values, $\epsilon_{initial}=1 \mu\text{m}$, $\epsilon_{final}=3 \text{ nm}$, $G=0.15 \text{ GeV/m}$, we obtain the length as a function of beam energy, as is shown in Fig. 4 for two different peak fields. The total accelerating voltage required is $V_{tot} = \log(\epsilon_{initial} / \epsilon_{final}) E / e$. The minimum length is reached at an energy where acceleration and damping sections are equal in length:

$$E_{optimum} = \sqrt{G/a} / \hat{B} \approx 340 \text{ T GeV} / \hat{B} \quad (6)$$

For this energy, the total length per main linac is

$$L_{tot} = 4 \log(\epsilon_{initial} / \epsilon_{final}) / \sqrt{aG} / \hat{B} \approx 52 \text{ km T} / \hat{B}$$

and the total voltage required is

$$V_{tot} = \log(\epsilon_{initial} / \epsilon_{final}) \sqrt{G/a} / (\hat{B}e) \approx 1.94 \text{ TV T} / \hat{B}$$

Table 3 lists example parameters for a peak field of 10 T; Fig. 5 illustrates how the equilibrium emittances depend on the field. Results with and without IBS are shown.

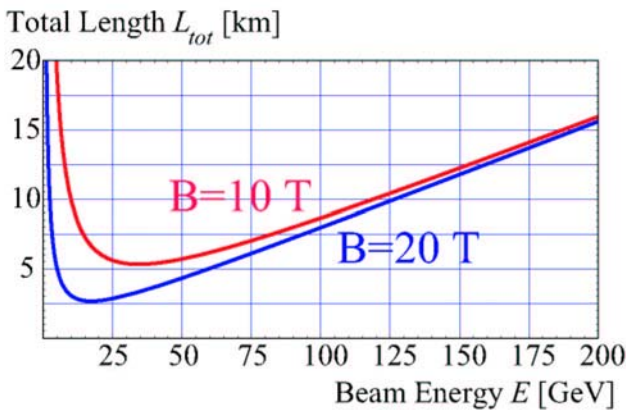


Figure 4: Length of damping section as a function of beam energy for wiggler peak fields of 10 and 20 T.

The final emittances vary linearly with the beta function. A FODO cell length of 6 m could accommodate 2 1.4 m long CLIC accelerating structures and 2 wiggler

units. Figure 6 depicts a possible optics, with $\langle \beta_{x,y} \rangle \approx 2.2, 8.4 \text{ m}$ average beta-functions at the wiggler. Quadrupoles could be 20 cm long, with 4-mm radius and 1.2-T pole-tip field.

Table 3: Example parameters for a sc linac wiggler.

Average beam energy	34 GeV
Peak magnetic field	10 T
Wiggler period	1.5 cm
Accelerating gradient	150 MV/m
Total length of wiggler/add'l. acceleration	2.6, 2.6 km
Average beta functions in wiggler	8, 1.5 m
Transverse damping time	1800 m/c
Equilibrium horizontal norm. emittance	400 nm
Equilibrium vertical norm. emittance	3.7 nm

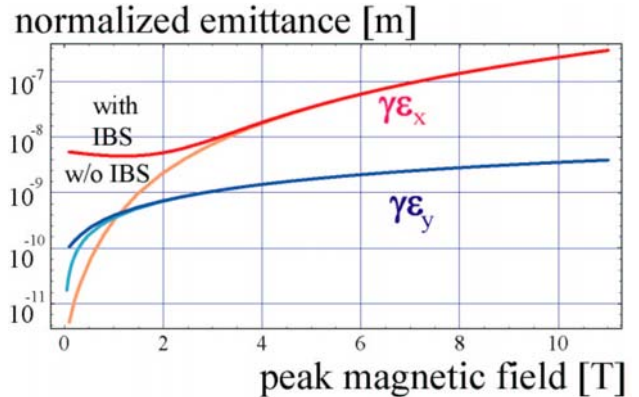


Figure 5: Normalized emittance from an sc linac-wiggler as a function of peak field at the optimized beam energy.

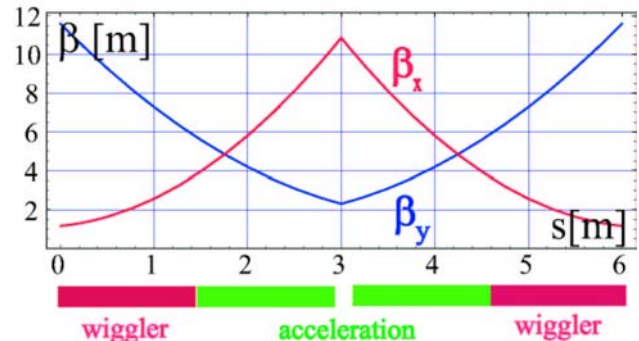


Figure 6: Example beta functions for wigglers interleaved with CLIC accelerating structures in the main linac.

REFERENCES

- [1] M. Korostelev, F. Zimmermann, Proc. Nanobeam'02 Lausanne and CERN-AB-2003-007-ABP (2003).
- [2] T. Shintake et al., Proc. Linac Conference, Tsukuba 1982, and Jap.J.Appl.Phys.21:L601-L603 (1982).
- [3] M. Seidel, DESY-TESLA-FEL-2001-08 (2001)
- [4] K. Hirata, SLAC AAS-Note 80 (1993).
- [5] A. Hofmann, SSRL ACD-Note 41 (1986).
- [6] Z. Huang, R.D. Ruth, PRL 80, 5, p. 976 (1998).
- [7] Z. Huang, Ph.D. Thesis SLAC-R-527 (1998).
- [8] K. Bane, Proc. EPAC2002 Paris (2002).
- [9] J.D. Bjorken, S.K.Mtingwa, Part. Acc. 13, 115 (1983).
- [10] N.Dikansky, A.Mikhailichenko, EPAC'92 (1992).